Geometric and Many-Particle Aspects of Transmitter Binding

Noam Agmon and Arieh L. Edelstein
Department of Physical Chemistry and the Fritz Haber Research Center, The Hebrew University, Jerusalem 91904 Israel

ABSTRACT We investigate the various reactivity patterns possible when several transmitter molecules, released at one side of a synaptic gap, diffuse and bind reversibly to a single receptor at the other end. In the framework of a one-dimensional approximation, the complete time, reactivity, concentration and gap-width dependence are determined, using a rigorous theoretical and computational approach to the many-body aspects of this problem. The time dependence of the survival probability is found to consist of up to four phases. These include a short delay followed by gaussian, power-law, and exponential decay phases. A rigorous expression is derived for the long-time exponent and approximate expressions are obtained for describing the short-time gaussian phase.

INTRODUCTION

One of the most extensively studied model systems for synaptic transmission is the nicotinic acetylcholine (Ach) receptor at the neuromuscular junction (Magleby and Stevens, 1972). An action potential at the presynaptic membrane triggers the exocytosis of synaptic vesicles. Each vesicle has a diameter of 25–50 nm and contains a few thousand Ach molecules. These are released into the synaptic cleft, ~50 nm wide, where they diffuse and are rapidly hydrolyzed by the enzyme acetylcholinesterase. Those Ach molecules reaching the post-synaptic (muscle) membrane may bind reversibly to a receptor (R). The receptor is a ligand-activated channel protein that has been isolated and characterized. It is constructed of five transmembranal subunits with a pore in its center. It most likely binds two Ach molecules noncooperatively at two different subunits. These binding events trigger a conformational change that opens a channel allowing sodium and potassium ions to cross the membrane. The release of a "quantum" of Ach by exocytosis of a single vesicle is sufficient for opening a few hundred ionic channels leading to a detectable "miniature end-plate current" (MEPC).

Since the work of Magleby and Stevens (1972), several groups have considered kinetic models as a quantitative description of the MEPCs (Rosenberry, 1979; Wathey et al., 1979; Land et al., 1981, 1984; Parnas et al., 1989; Buchman and Parnas, 1992; Friboulet and Thomas, 1993). These treatments mostly apply homogeneous chemical kinetics for describing the Ach-R binding step, although some include explicitly lateral (Wathey et al., 1979) or transversal (Friboulet and Thomas, 1993) Ach diffusion. The chemical kinetic description of a homogeneous bimolecular reaction assumes homogeneously distributed reactants in an infinite medium. This clearly does not describe the situation of a synaptic cleft of finite width, L, with receptors bound to the postsynaptic membrane (Friboulet and Thomas, 1993). Depending on conditions, the time course for binding may be different for these two problems.

As a simple example, consider a single Ach molecule with a single receptor. Formally, the reactants have equal concentrations so that bimolecular chemical kinetics will predict a hyperbolic time dependence with a $1/t$ approach to equilibrium. The true time dependence for binding depends on whether the receptor is static or mobile (Szabo et al., 1988) and whether the diffusion space is finite or infinite. If the receptor is static and the space infinite, the binding probability decays to zero as $t^{-d/2}$, where d is the spatial dimensionality (Pines et al., 1988; Agmon and Szabo, 1990). This behavior has been observed in fast (ps–ns) reversible geminate recombination in solution (Huppert et al., 1990). If space is finite and R static, the asymptotic approach to equilibrium is exponential. The smallest eigenvalue (in the exponent) may depend on the "intrinsic" binding and dissociation rate parameters for Ach-R at contact, and also on the Ach diffusion coefficient, D, and the interval length, L. If R also diffuses, L changes with time and the solution is again different.

When many Ach molecules are present, binding becomes competitive because only one Ach may be attached to a given binding site. The recombination rate parameter has a finite value, κ_r, only if the site is vacant. If the site is occupied, the recombination probability drops to zero. This competition effect couples the diffusive motion of the molecules, making reversible binding a truly many-body problem. Extensive work has been devoted to the understanding of this problem (Agmon and Szabo, 1990; Agmon et al., 1991; Agmon, 1993; Lee and Karplus, 1987; Vogelsang and Hauser, 1990; Burlatsky et al., 1991; Molski and Keizer, 1992; Naumann, 1993; Naumann and Molski, 1994; Molski and Naumann, 1994; Szabo, 1991; Szabo and Zwanzig, 1991; Richards and Szabo, 1991). When many receptors are considered, the binding at any given receptor may be coupled to binding at the other sites by mutual depletion of the Ach concentration. An array of receptors is expected to decrease the effective

Received for publication 14 September 1994 and in final form 16 December 1994.

Address reprint requests to Dr. Noam Agmon, Department of Physical Chemistry, Fritz Haber Research Center, The Hebrew University, Jerusalem 91904 Israel. Tel.: 972-2-585687; Fax: 972-2-513742; E-mail: agmon@batata.fh.huji.ac.il.

0006-3495/95/03/815/11 $2.00

lateral diffusion rate and diminish the probability that a dissociated ligand returns to the original receptor. Hence the binding process by itself is already extremely complicated.

In spite of the neglect of most of the abovementioned effects, it seemed possible to obtain a quantitative description of MEPCs by simple rate equations. One should recall that even with the inhibition of Ach-esterase, the electrophysiological signal is a convoluted response to (at least) three processes: (presynaptic) transmitter release, binding and (postsynaptic) channel gating. Unless the binding step is rate limiting, its transient details may make little difference to the MEPC. There may nevertheless be conditions (e.g., low Ach concentrations) where the transient binding kinetics do become rate limiting. In addition, there are numerous kinds of chemical synapses (e.g., in the central nervous system) and biochemical transmission systems (e.g., hormones) operating on the general principles of transmitter binding. Therefore it is important to find out how the binding probability depends on time, geometry, concentrations, interaction potentials, diffusion coefficient, etc. The goal of the present study is to start investigating these questions in a systematic way.

It is evident that such a detailed theoretical study of transmitter binding has to rely on simulation techniques. A few Monte Carlo simulations have been recently reported (Bartol et al., 1991; Faber et al., 1992), although these are geared mainly toward reproducing the MEPCs in the neuromuscular junction. We have recently developed a Brownian dynamics algorithm for reversible binding (Edelstein and Agmon, 1993), which has been applied to fast reactions in solution (Agmon and Edelstein, 1994; Edelstein and Agmon, 1994a, b). The essence of Brownian dynamics, as we see it, is that the exact single-particle distribution function is used to generate a single particle move. The Monte Carlo simulations of Bartol et al. (1991) apply this principle to free diffusion, when a particle is far from the receptor. We apply the same principle arbitrarily close to the reversible receptor, using the fact that the solution to the diffusion equation in one dimension and in the presence of a reversible trap is known analytically.

Provided the exact distribution function is used, an arbitrarily large time step may in principle be invoked without loss in accuracy. The approximation inherent in our application of Brownian dynamics is that while one particle moves the others remain static. The error in this approximation averages out after each particle makes just a few steps (Edelstein and Agmon, 1993). The ability to take large time steps is particularly important in biological systems. As discussed by Bartol et al. (1991), the microscopic time step for a single diffusive hop may be in the ps–ns time regime. It is impractical to use such small time steps to reach the μs–ms time regime. The Brownian algorithm allows one to investigate different time domains by varying the elementary time step. This is important in simulating biological processes, which may span many orders of magnitude in time.

The present study is mostly devoted to one-dimensional systems. Ach particles are released on one side of an interval (length L) that contains a single static reversible receptor on its other end. We investigate the dependence of the binding kinetics on the system size, L, and the number of particles, N. An exact transcendental equation is derived for the lowest eigenvalue (the observed rate coefficient) of the N-particle system. From this equation, simplified expressions for the rate coefficient may be obtained. Only their $L \to 0$ limit corresponds to conventional chemical kinetics.

We also investigate the applicability of one mean-field approximation, the superposition approximation (SA), for finite systems. This approximation has originally been applied for an infinite system in the thermodynamic limit (Lee and Karplus, 1987; Szabo and Zwanzig, 1991; Szabo, 1991). It may be adapted to arbitrary geometries when formulated as an effective single-particle diffusion equation with nonlinear boundary conditions (Agmon and Edelstein, 1994). Ultimately, the synaptic transmission problem with all its complexity may only be solvable through mean-field approximations. Establishing the validity of such mean-field approximations against exact Brownian simulations is another objective of this work.

THEORY

Problem definition

We consider the problem depicted schematically in Fig. 1. Two planar squares at $x = 0$ and $x = L$ represent post-and presynaptic membrane patches, respectively. We denote their area by a_M. On the first plane there is a reactive patch (the receptor) of area $a_R \leq a_M$ that can bind at most one particle reversibly. The analysis of a two-particle receptor is postponed to later work. On the presynaptic membrane, N particles (Ach molecules) are distributed randomly at $t = 0$. This initial planar δ-function may (or may not) depict the situation immediately following transmitter release from a presynaptic vesicle.

Because the two membranes are impermeable to Ach molecules on the time scale considered they are depicted as "reflective" planes. The receptor area becomes reflective only when a particle is bound to it. To avoid particle escape out

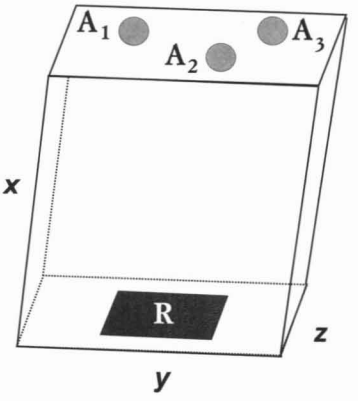

FIGURE 1 A schematic presentation of a small segment of a synaptic cleft. The presynaptic patch is depicted with three Ach transmitters, while the postsynaptic patch has a single receptor. The two membranes are separated by a gap of width L.

of the system we enclose it within a box with four reflective planes (parallel to the xy and xz planes). The unit cell in Fig. 1 repeats itself many times along the y and z directions. At short times particle exchange with neighboring cells is approximately balanced, so that the additional impermeable boundaries make little difference.

Starting from the given initial condition, the particles diffuse (diffusion coefficient D) within the volume $v = a_M L$ between the two membranes. We assume that they are noninteracting except at the "entrance" to the binding site. This amounts to neglecting the volume occupied by an Ach molecule and, for the time being, their Coulombic interactions. If a particle comes in contact with the receptor surface a_R, it can bind with a rate coefficient κ_r per unit area, provided that no other particle is bound. A bound particle may dissociate with a rate parameter κ_d to any point on receptor surface. κ_r has units of length/time, whereas κ_d has units of 1/time.

Consider the probability $q_1(t \mid \delta)$ that exactly one particle is bound to the receptor at time $t > 0$ having started from a planar δ-function distribution at $t = 0$. This "binding probability" is initially 0 and increases to an ultimate equilibrium level

$$q_1(\infty) = cK_{eq}/(1 + cK_{eq}), \tag{1}$$

which is, of course, independent of initial conditions. Here

$$c \equiv N/v = N/(a_M L) \tag{2}$$

is the overall particle concentration and

$$K_{eq} \equiv a_R \kappa_r/\kappa_d \tag{3}$$

is the (recombination) equilibrium coefficient. The question is how this limit is approached, namely, what is the time dependence of the "deviation from equilibrium", $q_1(\infty) - q_1(t \mid \delta)$.

The problem simplifies when the receptor occupies the whole postsynaptic patch, i.e., when $a_R = a_M$. The mixed boundary condition at the postsynaptic membrane is eliminated, so that neither the initial condition nor the boundary condition retain any yz dependence. The problem becomes one dimensional: N identical particles diffuse on the line segment $[0, L]$. The initial condition is a δ-function at $x = L$, and a reversible boundary condition is imposed at $x = 0$. The parameter κ_r is a recombination rate constant per unit area. Indeed, in the equilibrium limit discussed above, a_R and a_M cancel between Eqs. 2 and 3, so that $cK_{eq} = (N/L)(\kappa_r/\kappa_d)$. Thus $c \equiv N/L$ is a one-dimensional concentration and κ_r/κ_d a one-dimensional equilibrium coefficient.

The theory and Brownian simulations presented below correspond to this one-dimensional limit, where the receptor is "smeared out" over the postsynaptic membrane patch while keeping $a_R\kappa_r$ constant. The more general case $a_R \neq a_M$ is treated only in the framework of the mean-field SA at the very end of this work. It shows that the error inherent in the smearing-out assumption may not be very large.

Even when $a_R = a_M$, there are five parameters that determine the time evolution of the binding probability: κ_r, κ_d, D, L, and $c \equiv N/L$. Choosing time and distance scales sets the value of two parameters. Without loss of generality, one may set $\kappa_r = 1$ and $D = 1$. Thus, if t' and x' are the time and distance in given physical units, this choice amounts to transforming to the dimensionless variables

$$t \equiv \kappa_r'^2 t'/D', \qquad x \equiv \kappa_r' x'/D'. \tag{4}$$

The transient behavior of the binding probability will thus depend on three dimensionless parameters: L, κ_d, and c.

Many-particle equations

The many-particle equations (Agmon, 1993) describe the time evolution of the joint N-particle density $p(x_1, \cdots, x_N, t)$, where x_i is the distance of particle i from the receptor. When the receptor is vacant, all N particles diffuse independently

$$\frac{\partial p(x_1, \cdots, x_N, t)}{\partial t} = D \sum_{i=1}^{N} \frac{\partial^2}{\partial x_i^2} p(x_1, \cdots, x_N, t), \qquad 0 \le x_i \le L. \tag{5}$$

so that no coupling terms appear in this equation. The outer boundary conditions at $x_i = L$ are reflective

$$\frac{\partial}{\partial x_i} p(x_1, \cdots, x_N, t)\,|_{x_i = L} = 0, \qquad i = 1, \cdots, N. \tag{6}$$

The boundary conditions at the receptor ($x_i = 0$) represent a reversible reaction (Agmon, 1984). Using an asterisk to denote a bound particle, the binding of particle N, for example, is described by the flux at the boundary involving both recombination and dissociation terms

$$-D \frac{\partial}{\partial x_N} p(x_1, \cdots, x_N, t)\,|_{x_N = 0} = \kappa_d p(x_1, \cdots, x_{N-1}, *, t) - \kappa_r p(x_1, \cdots, x_{N-1}, 0, t). \tag{7}$$

Similar boundary conditions hold in $x_1, \cdots, x_{N-1}$.

While particle N is bound, the remaining $N - 1$ particles are free to diffuse. At the same time, particle number N may dissociate from or recombine with the receptor. Therefore

$$\frac{\partial p(x_1, \cdots, x_{N-1}, *, t)}{\partial t} = D \sum_{i=1}^{N-1} \frac{\partial^2}{\partial x_i^2} p(x_1, \cdots, x_{N-1}, *, t) + \kappa_r p(x_1, \cdots, x_{N-1}, 0, t) - \kappa_d p(x_1, \cdots, x_{N-1}, *, t). \tag{8}$$

Again, analogous equations hold if one of the other particles is bound.

The coupling between the N particles arises only because of the restriction that at most one particle is bound at any given time. Therefore the $N - 1$ particle density function obeys reflective boundary conditions at both ends of the interval

$$\frac{\partial}{\partial x_i} p(x_1, \cdots, x_{N-1}, *, t)\,|_{x_i = 0, L} = 0, \qquad i = 1, \cdots, N - 1, \tag{9}$$

and similarly when one of the other particles is bound. Thus, binding of a second particle is disallowed.

The structure of these N-particle equations is as follows. The independent motion of N particles on the line is isomorphic to the diffusion of a single point in N

dimensions. The N dimensional partial differential equation (Eq. 5) is coupled to N partial differential equations (Eq. 8) each of dimension $N-1$.

The quantity of experimental interest is the binding probability for a single particle, $q_1(t)$. When all N particles start from the same initial condition, e.g., all are initially randomly distributed on the presynaptic membrane,

$$p(x_1, \cdots, x_N, 0 \mid \delta) = \prod_{i=1}^{N} \delta(x_i - L), \tag{10}$$

the N functions obeying Eq. 8 become identical. The binding probability may then be obtained by integrating any one of them

$$q_1(t) = N \int_0^L \cdots \int_0^L p(x_1, \cdots, x_{N-1}, *, t)\, dx_1 \cdots dx_{N-1}. \tag{11}$$

The survival probability for a vacant trap is $S(t) \equiv 1 - q_1(t)$. Due to the finite size of the diffusion space it approaches an ultimate equilibrium value, $S_{eq} \equiv S(\infty)$.

The many-particle reaction rate

It may seem at first that the complexity of the N-particle equations precludes any kind of analytical treatment. Fortunately, this is not quite so. First, it is easily shown (Agmon, 1993) that the exact equilibrium value of the binding probability is given by Eq. 1. This follows because the lowest eigenfunction, with a corresponding zero eigenvalue, is the uniform distribution. The first excited eigenfunction, $\psi(x_1, \cdots, x_N)$, corresponds to the lowest nonvanishing eigenvalue λ. This eigenvalue determines the ultimate approach to equilibrium in the finite system and is thus the observed relaxation coefficient.

In a simple kinetic scheme

$$\mathrm{Ach} + \mathrm{R} \underset{\kappa_d}{\overset{\kappa_r}{\rightleftharpoons}} \mathrm{Ach} - \mathrm{R} \tag{12}$$

for acetylcholine-receptor binding and under the pseudo-unimolecular conditions, $c \equiv [\mathrm{Ach}] \gg [\mathrm{R}]$, the conventional chemical rate equations predict exponential approach to equilibrium with

$$\lambda = c\kappa_r + \kappa_d. \tag{13}$$

We will show that this value is approached only in the small-gap limit, $L \to 0$. In this limit the separation between eigenvalues becomes large, so that exponential kinetics dominates.

The first excited eigenfunction must possess a single node. Hence only the jth mode is excited, the remaining $N-1$ modes are uniformly distributed. Thus $\psi = \cos[\sqrt{\lambda/D}\,(L - x_j)]$, where $0 \le x_j \le L$. We symmetrize for identical particles by summing over all particles

$$\psi(x_1, \cdots, x_N) = \sum_{j=1}^{N} \cos[\sqrt{\lambda/D}\,(L - x_j)]. \tag{14}$$

The condition for ψ to have a single node is that

$$0 < L\sqrt{\lambda/D} \le \pi. \tag{15}$$

It is easy to check that ψ is an eigenfunction of the diffusion operator in Eq. 5,

$$D \sum_{i=1}^{N} \frac{\partial^2}{\partial x_i^2} \psi(x_1, \cdots, x_N) = -\lambda \psi(x_1, \cdots, x_N), \tag{16}$$

obeying $\partial\psi(x_1, \cdots, x_N)/\partial x_i|_{x_i = L} = 0$, as required by Eq. 6.

Note that ψ has an $N-1$ dimensional part that must be an eigenfunction of Eq. 8 with the same eigenvalue λ. Hence,

$$D \sum_{i=1}^{N-1} \frac{\partial^2}{\partial x_i^2} \psi(x_1, \cdots, x_{N-1}, *) + \kappa_r \psi(x_1, \cdots, x_{N-1}, 0) - \kappa_d \psi(x_1, \cdots, x_{N-1}, *) = -\lambda \psi(x_1, \cdots, x_{N-1}, *). \tag{17}$$

Similar relations hold, of course, in the other $N-1$ coordinates.

Let us integrate this equation over $x_1, \cdots, x_{N-1}$ and denote the corresponding integrals by $\bar{\psi}(*)$ and $\bar{\psi}(0)$. Due to exclusion of more than one-particle binding, Eq. 9, the integral of the second derivative in Eq. 17 vanishes and one obtains

$$\kappa_r \bar{\psi}(0) = (\kappa_d - \lambda)\bar{\psi}(*). \tag{18}$$

The parameter λ will now be determined from the back-reaction boundary condition at the receptor, Eq. 7. Integrating it and using the above identity gives

$$DL^{N-1} \left.\frac{\partial\psi(x_1, \cdots, x_N)}{\partial x_N}\right|_{x_N = 0} = \frac{\kappa_r \lambda}{\lambda - \kappa_d} \int_0^L \cdots \int_0^L \psi(x_1, \cdots, x_{N-1}, 0)\, dx_1 \cdots dx_{N-1}. \tag{19}$$

We have substituted the explicit expression for $\bar{\psi}(0)$ on the right-hand side (r.h.s.) The analogy with the Laplace transform in Eq. 3.4b of Agmon and Szabo (1990) is quite evident if the Laplace variable s is replaced by $-\lambda$.

Eq. 19 is the desired form of the boundary condition. Substituting ψ from Eq. 14 we finally obtain

$$\frac{\lambda - \kappa_d}{\kappa_r} = \sqrt{\frac{\lambda}{D}} \cot\left(\sqrt{\frac{\lambda}{D}}\, L\right) + \frac{N-1}{L}. \tag{20}$$

This transcendental equation holds for the first nonvanishing eigenvalue, provided that $0 < \sqrt{\lambda/D}\, L \le \pi$. Note that for a geminate pair, $N = 1$, the last term in Eq. 20 vanishes. If the reaction is additionally irreversible, then $\kappa_d = 0$ and Eq. 20 reduces to Eq. 4.9 in Agmon (1989).

Approximate many-particle reaction rates

Although Eq. 20 is exact, this transcendental equation does not resemble an expression for an effective rate coefficient of a multistep reaction. We bring it to a more familiar form by introducing an approximation. Using the partial-fraction expansion (Abramowitz and Stegun, 1970)

$$z \cot(z) \approx 1 + 2/(1 - \pi^2/z^2) + \cdots, \tag{21}$$

substituting and rearranging we find that

$$\lambda \approx \frac{(c\kappa_r + \kappa_d)\, D\pi^2/L^2}{(N+2)\kappa_r/L + \kappa_d + D\pi^2/L^2}, \tag{22}$$

where $c \equiv N/L$. In the limit of large N one has $N + 2 \approx N$, so that

$$\frac{1}{\lambda} \approx \frac{1}{c\kappa_r + \kappa_d} + \frac{L^2}{D\pi^2}. \tag{23}$$

This resembles a familiar recipe for the effective rate constant for reactions in series. In the present case the two consecutive steps are reversible, rather than irreversible. The first may be interpreted as a chemical step of binding and release. The second term on the r.h.s. represents a physical step of particle diffusion. The characteristic time, $1/\lambda$, for decay to equilibrium is the sum of the characteristic chemical and physical times.

In the large-gap limit ($L \to \infty$), the physical process is rate limiting and $\lambda \approx D\pi^2/L^2$. In the small-gap limit it is the chemical process that is rate limiting and $\lambda \approx c\kappa_r + \kappa_d$ (Eq. 13). This agreement with the chemical rate equations is somewhat superficial, even for small L. If $N \to 1$ the reaction is not pseudounimolecular, and ordinary rate equations predict a hyperbolic decay to equilibrium, whereas the exact solution is asymptotically exponential because of the finite system size, L. The two functions, $1/(1 + \lambda t)$ and $\exp(-\lambda t)$, agree only at short times. For large N the pseudounimolecular assumption holds but, as we shall see below, the time course of the reaction is then far from exponential.

The short-time behavior

So far we have derived exact and approximate expressions for the long-time exponential decay of the survival probability toward its ultimate equilibrium limit. The behavior need not be exponential over the whole time regime. Clearly, if the particles are initially at $x = L$, there would be a delay before they reach the receptor and begin binding. Whether the binding probability becomes exponential immediately thereafter depends on the values of L, c, and κ_d. We address this question by constructing a useful approximation for the short-time behavior.

In the model under investigation, particle-particle interactions arise only by competition over binding. Because initially the binding site is vacant, the short-time behavior is characterized by particles being independent of each other. This limit holds until particle-particle competition becomes appreciable. For independent particles, the probability of having no particle bound factors into a product of the probabilities that each individual particle is free.

Denote by $p(*, t \mid L)$ the single-particle binding probability, given that it was initially at $x = L$. It is the solution of Eqs. 5–10 for $N = 1$. The single-particle survival probability is $1 - p(*, t \mid L)$. The N-particle survival probability has this quantity to the power of N, giving for short times

$$S_{\text{short}}(t) = [1 - p(*, t \mid L)]^N \approx \exp[-Np(*, t \mid L)]. \tag{24}$$

The approximation on the r.h.s holds when $p(*, t \mid L) \ll 1$, which is also the condition for the independent-particle assumption to hold.

It is clear that Eq. 24 is not a good approximation at long times because it approaches the wrong equilibrium limit: given that $p(*, \infty) = K_{eq}/(L + K_{eq})$, set $N = 1$ in Eq. 1 (and $a_R = a_M$), then Eq. 24 gives $q_1(\infty) \approx cK_{eq}/(1 + cK_{eq}/N)$. For large N, this is considerably larger than the prediction from Eq. 1. The breakdown of the independent-particle approximation is due to the increasing role of the many-body competition effect.

An explicit form for $S_{\text{short}}(t)$ may be obtained by adopting a specific approximation for $p(*, t \mid L)$. For the problem at hand, there is a reflecting boundary condition at $x = L$, which defines the synaptic gap width. In the absence of this boundary (i.e., for a semi-infinite line), the single-particle binding probability is given analytically by Edelstein and Agmon (1993)

$$p_{\text{semi}}(*, t \mid L) = \frac{\kappa_r}{\Delta} e^{-L^2/4Dt} \left[\phi\left(\frac{L}{2\sqrt{Dt}} + \lambda_- \sqrt{t/D} \right) - \phi\left(\frac{L}{2\sqrt{Dt}} + \lambda_+ \sqrt{t/D} \right) \right]. \tag{25}$$

In the above equation, one defines

$$\lambda_\pm \equiv (\kappa_r \pm \Delta)/2, \qquad \Delta \equiv (\kappa_r^2 - 4D\kappa_d)^{1/2}, \qquad \phi(z) \equiv \exp(z^2)\text{erfc}(z). \tag{26}$$

erfc is the complementary error function.

The semi-infinite solution, $p_{\text{semi}}(x, t \mid L)$, is symmetrical around $x = L$ at short times. By reflecting its $x > L$ half at $x = L$ we obtain a short-time approximation for the solution with a reflecting boundary there. In this approximation, the binding probability in the absence of a reflecting boundary is simply multiplied by a factor of two, giving

$$S_{\text{short}}(t) \approx \exp[-2Np_{\text{semi}}(*, t \mid L)]. \tag{27}$$

This analytic approximation for the N-particle survival probability is expected to improve with decreasing κ_d. For large κ_d, the dissociating particles feel the presence of the outer reflecting boundary, which is absent in the approximate $p_{\text{semi}}(*, t \mid L)$.

To obtain a better feeling for the behavior of the short-time approximation in Eq. 27, let us simplify the analytical expression in Eq. 25 using the simplest rational approximation for the error function (Abramowitz and Stegun, 1970)

$$\phi(z) \approx 1/(1 + \alpha z). \tag{28}$$

The choice of α depends on the expected range of z values

$$\alpha = \begin{cases} 2/\sqrt{\pi}, & \text{small } z, \\ \sqrt{\pi}, & \text{large } z. \end{cases} \tag{29}$$

The small-z approximation reproduces the first two terms in the small-z expansion. The large-z approximation reproduces the leading terms in both $z = 0$ and $z \to \infty$ limits.

Using approximation 28 in Eq. 27 we obtain

$$\ln S_{\text{short}}(t) \approx -\frac{2N\alpha\kappa_r\sqrt{t/D}\, e^{-L^2/4Dt}}{1 + \alpha\left(\frac{L}{\sqrt{Dt}} + \kappa_r\sqrt{t/D}\right) + \alpha^2\left(\frac{L^2}{4Dt} + \frac{L\kappa_r}{2D} + \kappa_d t\right)}, \tag{30}$$

where α is chosen as in Eq. 29.

The above result helps characterize the short-time behavior of the survival probability. For small t, we have

that $\ln S(t) \approx 0$. For larger t but negligible κ_d, the denominator reads $\alpha\kappa_r\sqrt{t/D}$. In this regime $\ln S_{short}(t) \approx -2N \exp[-L^2/4Dt]$. At still longer times, the approximations leading to Eq. 27 breakdown.

Using the above simple analysis, we conclude that for slow dissociation the time dependence of $\ln S(t)$ has four different phases. At times shorter than the delay time for crossing the gap it vanishes. Thereafter it resembles a gaussian that is proportional to N. At infinitely long times there is linear decay, the slope being the eigenvalue λ from Eq. 20. The transition between the gaussian and linear decay phases occurs through a power-law regime, which becomes important for large L.

RESULTS

Using numerical methods, we investigated the transient behavior of the survival probability, $S(t \mid \delta) = 1 - q_1(t \mid \delta)$, in one dimension for a reversible binding site at the origin with N randomly moving particles initially at $x = L$. Time and distance units are such that the recombination parameter, κ_r, and the particle diffusion coefficient, D, are unity. The complete time dependence was calculated for different values of the dissociation parameter κ_d, the interval length L, and the concentration $c \equiv N/L$.

Two numerical methods were used, as discussed in Edelstein and Agmon (1993). For $N = 1$–3 the exact solution of the coupled partial differential Eqs. 5–9 was obtained by direct propagation. In this method, the temporal propagator is expanded in the uniformly converging Chebyshev polynomials allowing large time steps with high accuracy. The probability density, calculated with double precision accuracy, was used in Eq. 11 for obtaining the survival probability. For more than three particles, direct propagation is impractical because of large memory requirements. In this case we utilize Brownian dynamics for generating a huge number of stochastic trajectories. Each trajectory is obtained by moving a single particle at a time, using an analytic single-particle solution for reversible binding in one dimension. The binding probability is averaged over the ensemble of stochastic trajectories. The total of over a year in continuous 486 PC runs was required to reduce the statistical noise to acceptable limits. For small N, we checked that the two methods agree to within the statistical error of the Brownian dynamics results.

This section is divided into four parts. First, small-gap ($L \to 0$) propagations are presented and used as a check of our expressions for the first nonvanishing eigenvalue. Then we discuss the large-gap results, obtained by Brownian dynamics, and exemplify the short-time gaussian behavior. Subsequently, we demonstrate the concentration effect on the binding kinetics. Finally we present a calculation using experimentally accepted parameters for the Ach neuromuscular junction and demonstrate the effect of varying receptor area in a three-dimensional approximation.

Narrow-gap limit

Fig. 2 demonstrates the approach to equilibrium on a (natural) semilogarithmic scale. The results, obtained by direct propagation, involve no statistical noise. The concentration is fixed, $c = 0.4$, while the number of particles N and the gap-width L increase proportionately from left to right. In each panel, the dissociation parameter κ_d is varied over five orders of magnitude. To differentiate between the five curves, the deviation from equilibrium is divided by cK_{eq}. The figure shows that in this limit, the transient behavior is characterized by a short delay followed by exponential decay.

The delay is roughly the time required for the mean-square displacement to equal half the gap width

$$t_{delay} \approx L^2/8D. \quad (31)$$

During this delay time the survival probability hardly changes. At later times, the approach to equilibrium becomes exponential as evident from the straight lines in Fig. 2. Their slopes at large t, obtained by linear regression, are presented as open symbols in Fig. 3. They should be equal to the first nonvanishing eigenvalue λ.

The crosses show λ as calculated numerically from the transcendental Eq. 20. Some care is exercised, because the two sides are quite sensitive functions of λ. The agreement with the direct propagation results (open symbols) is generally very good. For large L and small κ_d, the eigenvalue spectrum becomes more congested, which is probably the reason that the direct propagation slopes slightly overestimate the lowest eigenvalue, λ.

The approximate analytical expression in Eq. 22 is demonstrated by the full curves. It nicely interpolates between the large-κ_d limit, $D\pi^2/L^2$, and a value smaller by a factor $1/[(N + 2)/N + D\pi^2/c\kappa_r L^2]$ obtained in the limit of vanishing κ_d. In the thermodynamic limit of large N and L, this factor approaches unity, and the lowest eigenvalue shows only a slight dependence on κ_d. Indeed, a particle that is nearly always unbound behaves like a particle in a box of length L, whose lowest nonvanishing eigenvalue is $D\pi^2/L^2$. In our dimensionless units, this holds when either $\kappa_d \to \infty$ or else both N and L are large. In these cases λ is mainly a measure of the physical dimensions of the

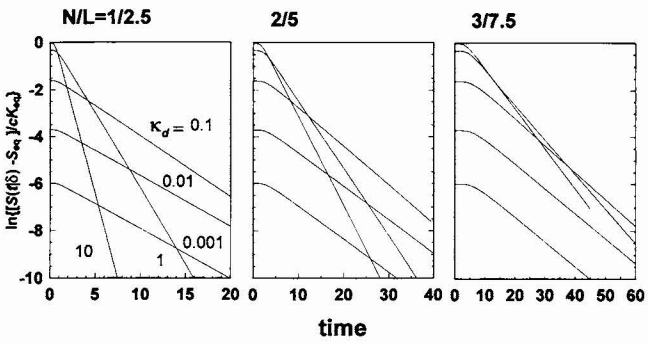

FIGURE 2 The approach to equilibrium in the small-gap limit for $c = 0.4$, using the direct propagation method. Values for N, L, and κ_d are indicated.

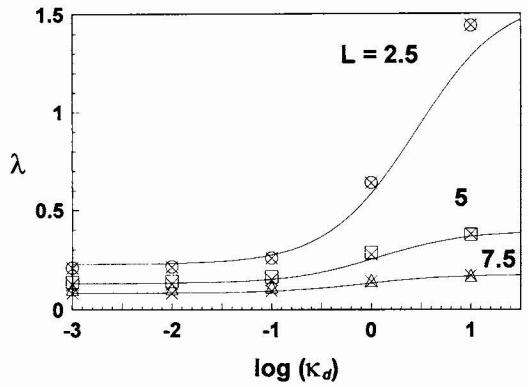

FIGURE 3 The lowest nonvanishing eigenvalue for $c = 0.4$. (○, □, △) Long-time slopes obtained from Fig. 2 for $N = 1$, 2, and 3, respectively. Crosses are numerical solutions to Eq. 20. Lines are from Eq. 22.

gap, rather than of the chemical binding and unbinding rate parameters. It is only in the small-gap small-κ_d limit that the chemical binding parameters determine the observed kinetics.

Wide-gap limit

The survival probability for reversible binding in one dimension with an initial δ-function condition has been calculated in the large-gap limit using Brownian dynamics. Results, shown as bold curves in Fig. 4, cover the whole time regime, from short times and up to the ultimate equilibrium limit, S_{eq}, accurately depicted by Eq. 1. It depends on concentration and binding parameters, but not on N and L separately. Hence the same asymptotic limits are approached in all three panels. S_{eq} is evidently closer to unity for larger κ_d.

Short-time behavior

Unlike the situation in the narrow-gap limit, the short-time behavior after the initial delay is not exponential. One may compare the results in Fig. 4 to the theoretical predictions. The independent-particle approximation, Eq. 24, is demonstrated by the dashed curves. To obtain these curves, we have evaluated numerically the single-particle binding probability, $p(*, t \mid L)$, using direct propagation. This solution is subject to the same initial and boundary conditions as the many-particle problem it approximates. The approximation in Eq. 24 is seen to reproduce the steep decay observed at short times. At intermediate and longer times it underestimates the exact survival probability, as discussed after Eq. 24. The time when the two solutions first deviate may be viewed as the onset of coupled many-particle dynamics.

An approximate independent particle solution was obtained by eliminating the reflecting boundary at $x = L$, replacing $p(*, t \mid L)$ by twice the analytical solution for a semi-infinite line, $p_{semi}(*, t \mid L)$, Eq. 25. Small L is the worst case for this approximation because particles leaving the binding site may feel the absence of the reflecting boundary. We therefore demonstrate the approximation in Eq. 27 for the narrowest gap, $L = 25$ (dotted curves). For small κ_d the agreement between the dashed and dotted curves is excellent. It deteriorates for larger κ_d, when particles have a larger chance to unbind and migrate to the (missing) outer boundary.

Our final approximation involved the rational approximation leading to the gaussian approximation in Eq. 30. It is shown by the dash-dotted curves for $L = 250$. Because for large L the argument of $\phi(z)$ is large, we use $\alpha = \sqrt{\pi}$ in Eq. 28. The agreement demonstrates that the initial decay phase of $\ln S(t)$ is indeed gaussian. For small κ_d it is given by $\ln S_{short}(t) \approx -2N \exp(-L^2/4Dt)$. This initial behavior is linearly amplified with N. It represents the effect of a "swarm" of particles arriving at the receptor site.

Long-time behavior

The long-time behavior in the approach to equilibrium is better appreciated when represented as the (scaled) deviation from equilibrium, $[S(t \mid \delta) - S_{eq}]/cK_{eq}$ (see Fig. 5). Note how after subtraction of the equilibrium limit, the statistical noise in the Brownian simulations becomes more apparent. The exact solutions are compared with the SA as described in

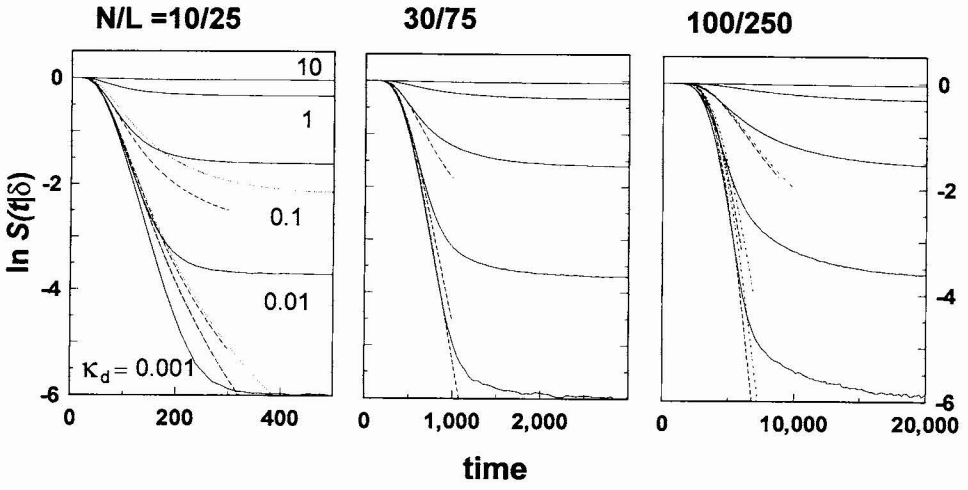

FIGURE 4 The time dependence of the survival probability in the wide-gap limit for $c = 0.4$ and the indicated values of N, L, and κ_d. Full curves are Brownian simulations. Dashed curves are the independent-particle approximation, Eq. 24. Dotted curves for $L = 25$ (left panel) are from Eq. 27. Dash-dotted curves for $L = 250$ (right panel) are from Eq. 30.

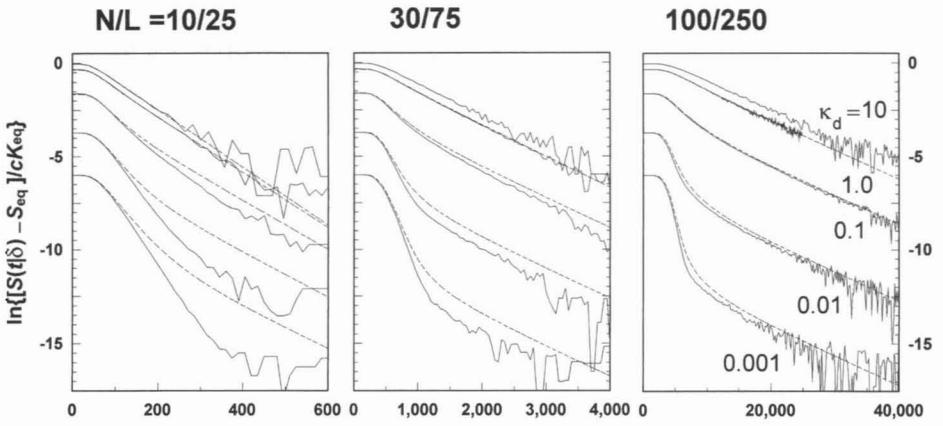

FIGURE 5 The deviation from equilibrium obtained by subtracting the equilibrium limit from the data in Fig. 4. Full curves are Brownian simulations. Dashed curves are an application of the superposition approximation to a system of finite size (Agmon and Edelstein, 1994).

Agmon and Edelstein (1994). This approximation tends to the correct equilibrium plateau only in the thermodynamic limit of an infinite system ($L \to \infty$). Thus, to obtain the dashed curves in Fig. 5 we subtract the approximate S_{eq} values. Unlike the independent-particle approximation described above, the superposition is capable of reproducing both short- and long-time behaviors. It becomes really useful near the thermodynamic limit, when both N and L are large.

As is also seen from this semi-log plot, the asymptotic approach to equilibrium for a finite gap width is always exponential and governed by the lowest eigenvalue λ. Unlike the narrow-gap limit, where the exponential phase encompasses most of the observed behavior, in the wide-gap limit it is really only asymptotic. The asymptotic regime extends to shorter times with increasing κ_d. Indeed, in this limit the denominator of Eq. 30 becomes large, so that the amplitude of the gaussian phase diminishes. What remains in this limit is mostly the exponential decay.

The slope in the large κ_d limit should approach, according to Eqs. 20 or 22, the particle-in-a-box limit, $\lambda \approx D\pi^2/L^2$. Fig.6 collects the long-time slopes for $\kappa_d = 10$ obtained by linear regression in both Figs. 2 and 5 for $N = 1$–100. The agreement with $\lambda \approx D\pi^2/L^2$ is perfect. Thus for fast dissociation, the data contain no information on the chemical binding coefficients, irrespective of the gap width.

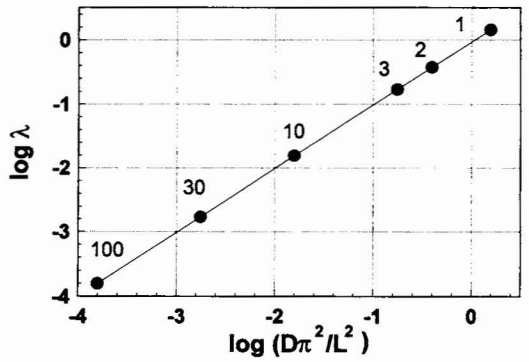

FIGURE 6 The long-time exponent for $c = 0.4$ and $\kappa_d = 10$ as obtained by linear regression in Figs. 2 and 5. The values of N are indicated. L is such that $N/L = c = 0.4$. The linear regression line has a slope of unity.

For smaller κ_d values in the wide-gap limit one observes a turnover from the short-time gaussian decay to the long-time exponential decay. As $L \to \infty$, this turnover regime develops into a power-law behavior. To see this, we show in Fig. 7 some of our data in a (natural) log-log scale. In the slow dissociation limit, $\kappa_d = 0.001$, a linear regime is observable at intermediately long times. This regime is seen most clearly for the widest gap, $L = 250$, around $\ln t = 9$–10. As the thermodynamic limit of an infinite system is approached, this phase develops into the well-known $t^{-d/2}$ asymptotic behavior, d being the dimensionality of the diffusion space (Szabo and Zwanzig, 1991; Agmon and Edelstein, 1994).

As a reference, we show in the figure our previous thermodynamic-limit results (Agmon and Edelstein, 1994) for an "infinite" system with a uniform initial distribution

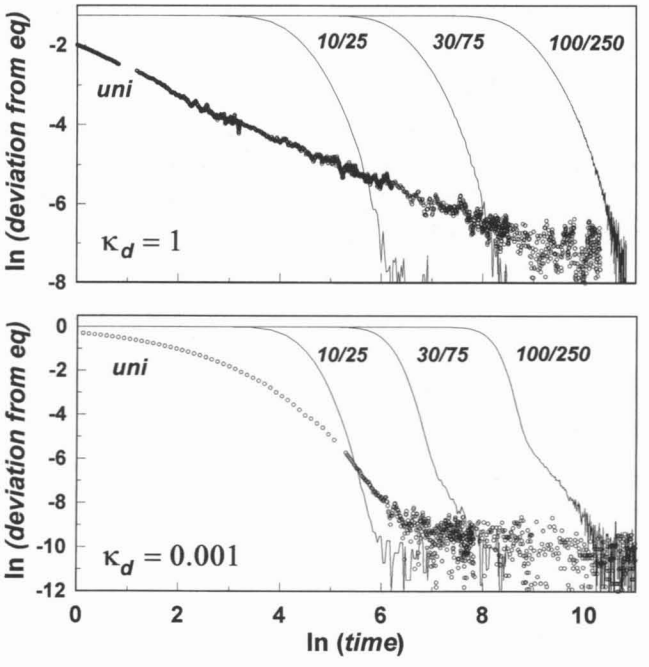

FIGURE 7 Comparison of the approach to equilibrium for an initial δ function and a finite system (N/L values indicated) with an initial uniform distribution and a semi-infinite line (○). $c = 0.4$ and κ_d is indicated in each panel. Note the ln-ln scale.

(circles). The change in geometry and initial conditions has a profound effect on the observed behavior. For example, in the large κ_d limit uniformly distributed particles lead to predominantly power-law decay while the δ-function distribution considered here results in a predominantly exponential approach to equilibrium.

Concentration effects

Results so far were restricted to a fixed concentration. The parameters varied were L and κ_d. To investigate the concentration effect, we have repeated the calculations of Fig. 5 twice, for concentrations that are a factor of 10 smaller and larger. These results are collected in Fig. 8. The figure contains six panels, with L varying horizontally and c varying vertically from panel to panel. As before, κ_d is varied within each panel. These results were obtained by Brownian simulations except for the two panels with $c = 0.04$ and $L = 25$ and 75.

The binding kinetics demonstrated by Fig. 8 cover the different possible behaviors. In all cases there is a short delay phase and a long-time exponential approach to equilibrium. As either L or c are increased, one observes the appearance of the two intermediate phases: the gaussian decay of $\ln S(t)$ and the power-law transition region between the gaussian and exponential regimes. These different behaviors have been discussed in detail above. Thus as c is decreased the narrow-gap behavior extends to larger values of L, while when it is increased, the wide-gap behavior extends to smaller L values.

The neuromuscular junction

Having analyzed the behavior of the binding probability over the entire parameter range, let us consider a biophysical example of the Ach-receptor at the neuromuscular junction. There is a more or less accepted set of parameters in the literature (Land et al., 1981, 1984; Friboulet and Thomas, 1993). Using primes to denote quantities with physical units, we take $L' = 50$ nm, $a_M = 49$ nm^2, $a_R = 1$ nm^2, $\kappa_r' = 10^8$ M^{-1}s^{-1} ≈ 100 nm^2/(particle $\cdot$ μs), $\kappa_d' = 0.01$ μs^{-1}, $D' = 200$ nm$^2/\mu$s and $N = 3$. Here a_M is the average membrane area per receptor, whose active site occupies the smaller area a_R. Thus we assume that a box of dimensions $7 \times 7 \times 50$ nm contains a single receptor on the postsynaptic side with about three Ach molecules released at the presynaptic side.

As discussed in the Problem Definition section, the problem becomes one-dimensional if $a_R = a_M$. We therefore "smear" the active site so it occupies the whole postsynaptic patch, keeping $a_R\kappa_r'$ constant. Increasing a_R to 49 nm^2 we decrease κ_r' to 2.04 nm^2/(particle $\cdot$ μs). In the dimensionless units in which $D = \kappa_r = 1$ (Eq. 4), we have $L = 0.51$, $\kappa_d = 0.48$, and $c = 5.9$. When compared with our previous calculations, one expects the binding kinetics to be in the small-gap limit.

Fig. 9 shows the normalized deviation from equilibrium, $[S(t \mid \delta) - S_{eq}]/(1 - S_{eq})$, for the above parameters. Both Brownian dynamics and direct propagation produce the same outcome. As expected, it shows only the short-time delay and the long-time exponential decay characteristic of systems in the narrow-gap limit. The slope and the solution of the transcendental Eq. 20 give $\lambda' = 0.11$ μs. The approximation in Eq. 22 gives $\lambda' = 0.105$ μs while $c'\kappa_r' + \kappa_d' = 0.13$ μs. Thus, using a simple kinetic approach introduces little error in this case.

Finally, we have investigated the effect of eliminating the one-dimensionality constraint in the context of the SA. As seen in Fig. 5, this approximation becomes less accurate in the small L limit. The dashed curve in Fig. 9 agrees with the initial 80% of the exact one-dimensional decay. We compare

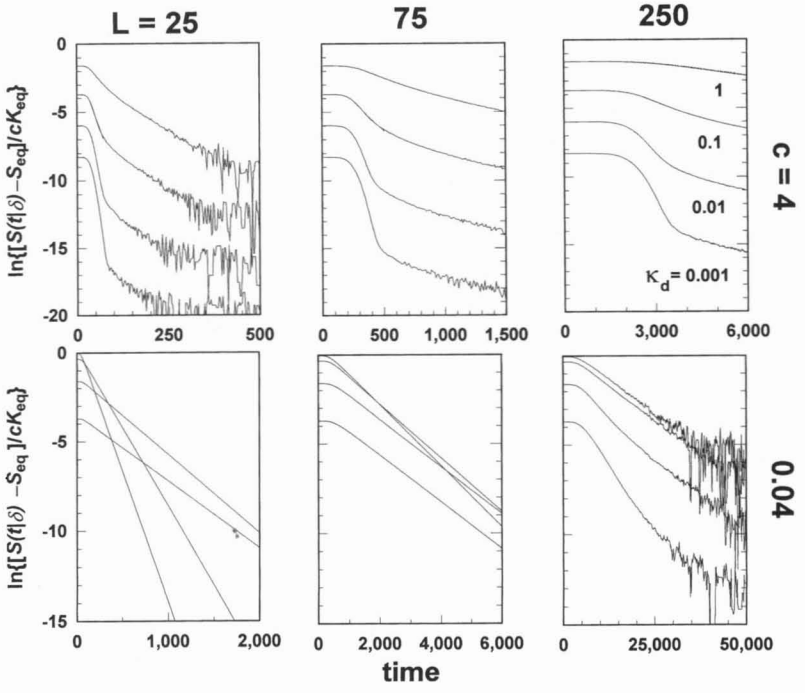

FIGURE 8 Concentration, gap-width, and reactivity effects on competitive reversible binding starting from a δ-function distribution.

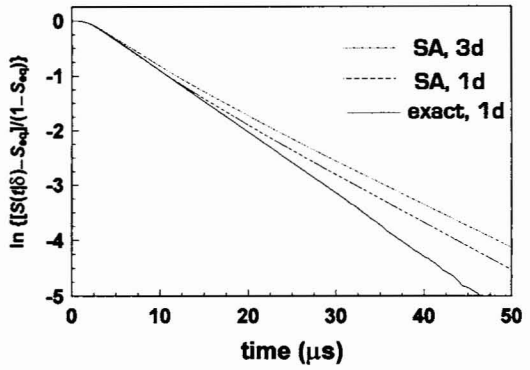

FIGURE 9 Receptor binding kinetics using experimental parameters for the neuromuscular junction.

it with a full three-dimensional calculation in which a_R is reduced to its original area, about $a_M/50$ (dash-dotted curve). As could be expected, the introduction of a mixed boundary condition at the postsynaptic membrane slows down the binding process. This resembles a "steric effect" on chemical reactivity, arising from nonproductive collisions with the nonreactive fraction of the postsynaptic membrane.

CONCLUSION

In several important biophysical situations, such as neurotransmittance across a synaptic junction, particles diffuse across a finite gap and bind reversibly to a receptor at its other end. To our knowledge, the present work is the first rigorous analysis of many-body effects on this process, albeit within a one-dimensional approximation. We find that the general time behavior of the receptor's survival probability consists of four phases: a short delay followed by gaussian, power-law, and exponential decay phases. The relative weight of each phase depends on the exact value of the binding parameters, particle concentration and gap width. This work reports a systematic investigation of the effect of their variation.

Qualitatively speaking, the four phases are the combined effect of the restricted geometry, the many-particle competition over binding, and the δ-function initial condition. The delay time is required for crossing the gap. The gaussian phase signals the arrival of a "swarm" of particles at the receptor. The power-law phase appears when particle-binding events are no longer independent, and the asymptotic exponential phase reflects the series addition of "physical" gap crossing and "chemical" binding.

We employed both numerical and analytical theory to reach these conclusions. The two numerical methods utilized in the calculations are direct propagation, applicable to a small number of particles, and Brownian dynamics, for simulating many particles over extended time regimes. A rigorous expression, Eq. 20, was derived for the long-time exponent, and approximate expressions were obtained for the transient behavior in the short-time gaussian phase. These results were found to agree nicely with our calculations.

It is interesting that most previous neurobiological work has assumed simple chemical rate laws for the many-particle diffusion and binding events. This assumption has not been justified by more rigorous analyses. In retrospect, we find that simple chemical kinetics may not be in great error for the experimental conditions in the neuromuscular junction. It is nevertheless clear that the richness of behaviors inherent in this problem far exceeds the simplistic kinetic limit. Many of these effects may be captured by mean-field approximations such as the SA, which can be solved numerically in three dimensions for general geometries. Bearing in mind the multitude of intercellular signaling mechanisms, it is interesting to see whether the different limits observed in this study could be realized in model experimental systems.

It is a pleasure to acknowledge discussions, correspondence and comments from R. S. Eisenberg, W. Naumann, H. Parnas and E. E. Salpeter. Work was supported by grants from the Absorption Ministry (A.L.E.) and from the US-Israel Binational Science Foundation, Jerusalem, Israel (N.A.). The Fritz Haber Research Center is supported by the Minerva Gesellschaft für die Forschung, München, Germany.

REFERENCES

Abramowitz, M. and I. A. Stegun, editors. 1970. Handbook of Mathematical Functions. Dover Publications, New York.

Agmon, N. 1984. Diffusion with back-reaction. *J. Chem. Phys.* 81:2811–2817.

Agmon, N. 1989. Viscosity expansions in reactive diffusion processes. *J. Chem. Phys.* 90:3765–3775.

Agmon, N. 1993. Competitive and non-competitive reversible binding processes. *Phys. Rev. E.* 47:2415–2429.

Agmon, N., and A. L. Edelstein. 1994. The long-time behavior of reversible binary reactions: theory, Brownian simulations and experiment. *J. Chem. Phys.* 100:4181–4187.

Agmon, N., H. Schnörer, and A. Blumen. 1991. Competitive reversible binding: a bimolecular boundary condition for the diffusion equation. *J. Phys. Chem.* 95:7326–7330.

Agmon, N., and A. Szabo. 1990. Theory of reversible diffusion-influenced reactions. *J. Chem. Phys.* 92:5270–5284.

Bartol, T. M. Jr., B. R. Land, E. E. Salpeter, and M. M. Salpeter. 1991. Monte Carlo simulation of miniature endplate current generation in the vertebrate neuromuscular junction. *Biophys. J.* 59:1290–1307.

Buchman, E., and H. Parnas. 1992. Sequential approach to describe the time course of synaptic channel opening under constant transmitter concentration. *J. Theor. Biol.* 158:517–534.

Burlatsky, S. F., G. S. Oshanin, and A. A. Ovchinnikov. 1991. Kinetics of chemical short-range ordering in liquids and diffusion-influenced reactions. *Chem. Phys.* 152:13–21.

Edelstein, A. L., and N. Agmon. 1993. Brownian dynamics simulations of reversible reactions in one dimension. *J. Chem. Phys.* 99:5396–5404.

Edelstein, A. L., and N. Agmon. 1994a. Brownian dynamics of reversible binding processes. *In* Ultrafast Reaction Dynamics and Solvent Effects. Y. Gauduel and P. J. Rossky, editors. AIP Conference Proceedings 298, New York. 473–484.

Edelstein, A. L. and N. Agmon. 1994b. Equilibration in reversible bimolecular reactions. *J. Phys. Chem.* In press.

Faber, D. S., W. S. Young, P. Legendre, and H. Korn. 1992. Intrinsic quantal variability due to stochastic properties of receptor-transmitter interactions. *Science.* 258:1494–1498.

Friboulet, A., and D. Thomas. 1993. Reaction-diffusion coupling in a structured system: application to the quantitative simulation of endplate currents. *J. Theor. Biol.* 160:441–455.

Huppert, D., E. Pines, and N. Agmon. 1990. Long-time behavior of reversible geminate recombination reactions. *J. Opt. Soc. Am. B.* 7:1545–1550.

Land, B. R., W. V. Harris, E. E. Salpeter, and M. M. Salpeter. 1984. Diffusion and binding constants for acetylcholine derived from the falling phase of miniature endplate currents. *Proc. Natl. Acad. Sci. USA.* 81:1594–1598.

Land, B. R., E. E. Salpeter, and M. M. Salpeter. 1981. Kinetic parameters for acetylcholine interaction in intact neuromuscular junction. *Proc. Natl. Acad. Sci. USA.* 78:7200–7204.

Lee, S., and M. Karplus. 1987. Kinetics of diffusion-influenced bimolecular reactions in solution. I. General formalism and relaxation kinetics of fast reactions. *J. Chem. Phys.* 86:1883–1903.

Magleby, K. L., and C. F. Stevens. 1972. A quantitative description of end-plate currents. *J. Physiol.* 223:173–197.

Molski, A., and J. Keizer. 1992. Kinetics of nonstationary, diffusion-influenced reversible reactions in solution. *J. Chem. Phys.* 96:1391–1398.

Molski, A., and W. Naumann. 1994. Monomer-excimer kinetics in solution. II. Statistical nonequilibrium thermodynamic approach. *J. Chem. Phys.* 100:1520–1527.

Naumann, W. 1993. The reversible reaction A + B = C in solution: a system-size expansion approach on the base of reactive many-particle diffusion equations. *J. Chem. Phys.* 98:2353–2365.

Naumann, W., and A. Molski. 1994. Monomer-excimer kinetics in solution. I. Stochastic many-particle approach. *J. Chem. Phys.* 100:1511–1519.

Parnas, H., M. Flashner, and M. E. Spira. 1989. Sequential model to describe the nicotinic synaptic current. *Biophys. J.* 55:875–884.

Pines, E., D. Huppert, and N. Agmon. 1988. Geminate recombination in excited-state proton transfer reactions: numerical solution of the Debye-Smoluchowski equation with back-reaction boundary conditions. *J. Chem. Phys.* 88:5620–5630.

Richards, P. M., and A. Szabo. 1991. Reversible trapping on a cubic lattice: comparison of theory and simulations. *J. Stat. Phys.* 65:1085–1093.

Rosenberry, T. 1979. Quantitative simulation of endplate currents at neuromuscular junctions based on the reaction of acetylcholine with acetylcholine receptor and acetylcholinesterase. *Biophys. J.* 26:263–290.

Szabo, A. 1991. Theoretical approaches to reversible diffusion-influenced reactions: monomer-excimer kinetics. *J. Chem. Phys.* 95:2481–2490.

Szabo, A., and R. Zwanzig. 1991. Reversible diffusion influenced reactions: comparison of theory and simulation for a simple model. *J. Stat. Phys.* 65:1057–1083.

Szabo, A., R. Zwanzig, and N. Agmon. 1988. Diffusion controlled reactions with mobile traps. *Phys. Rev. Lett.* 61:2496–2499.

Vogelsang, J., and M. Hauser. 1990. Strong transient effects of nonstationary diffusion on excimer formation. Test of the concept of convolution kinetics. *J. Phys. Chem.* 94:7488–7494.

Wathey, J. C., M. M. Nass, and H. A. Lester. 1979. Numerical reconstruction of the quantal event at nicotinic synapses. *Biophys. J.* 27:145–164.